Supplemental information

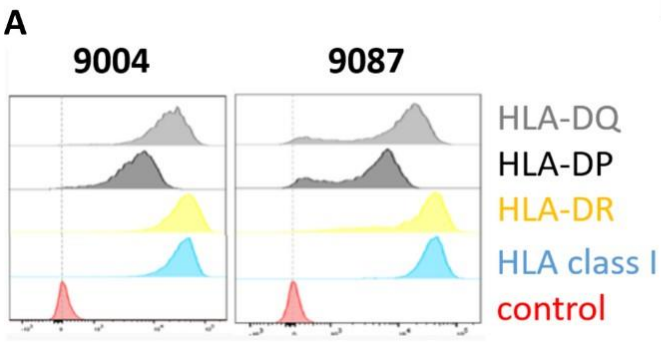

B

BLCL 9004		BLCL 9087	
Allele	Global Freq.	Allele	Global Freq.
HLA-A*02:01	15.3%	HLA-A*01:01	4.8%
HLA-B*27:05	1.2%	HLA-B*08:01	3.0%
HLA-C*01:02	8.5%	HLA-C*07:01	6.9%
DRB1*01:01	4.1%	DRB1*03:01	6.8%
DQA1*01:01	12.7%	DQA1*05:01	26.0%
DQB1*05:01	9.3%	DQB1*02:01	15.0%
DPA1*01:03	58.3%	DPA1*01:03	58.3%
DPB1*04:01	23.3%	DPB1*03:01	6.6%
		DPB1*04:01	23.3%

Supplemental Figure S1. Flow cytometric analysis and HLA typing of BLCL. (A) BLCL were stained with SPV-L3 (HLA-DQ), B7/21 (HLA-DP), LB3.1 (HLA-DR) or W6/32 (pan-HLA class I) antibodies to assess HLA expression. Histogram plots are gated on live cells, representative of >10 independent experiments. Control cells were stained with secondary detection antibody only. **(B)** HLA haplotypes of BLCL cells chosen for this study, including the global occurrence frequency for each allotype (from pypop.org based on [1]).

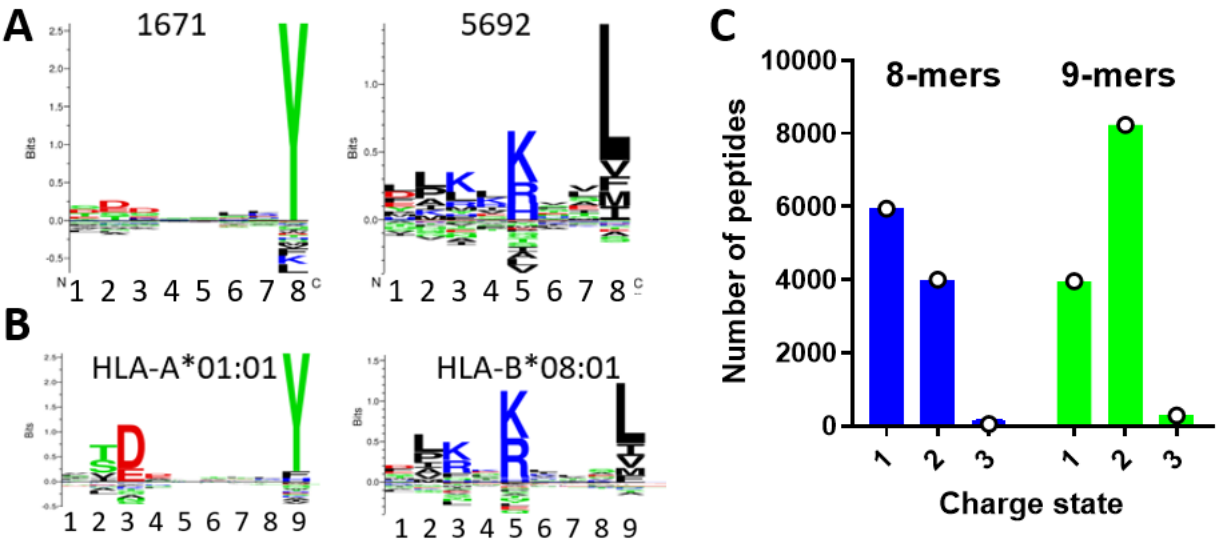

Supplemental Figure S2. Properties of 8-mers in 9087 BLCL. (A) Gibbs clustering analysis of 8-mers including the number of peptides allocated to each cluster. (B) NetMHC derived motif for HLA-A*01:01 and HLA-B*08:01 which are expressed by 9087. (C) Detected peptide numbers and their charge state for 8 and 9 amino acid long peptides (blue and green, respectively). A representative class I elution of 9087 BLCL transfected with Protein E is shown.

A

Posttranslational Modification	Count
Oxidation (M)	22
Deamidation (NQ)	7
Dehydration	6
Acetylation (N)	4
Cysteinylation	2
Formylation	2
Oxidation (HW)	2
Pyro-glu from E	2
Biotinylation; Acetylation (K)	1
Beta-methylthiolation	1
Cysteine oxidation to cysteic acid	1
Phosphorylation (STY); Ethanolation (C)	1
Tryptophan oxidation to kynurenin	1
Ammonia-loss (N)	1

B

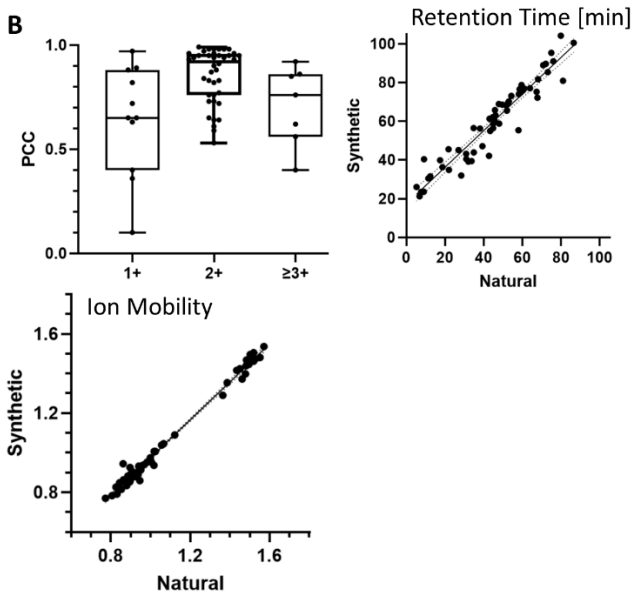

C. Mirror plots of acquired natural (top) vs synthetic (bottom) peptides

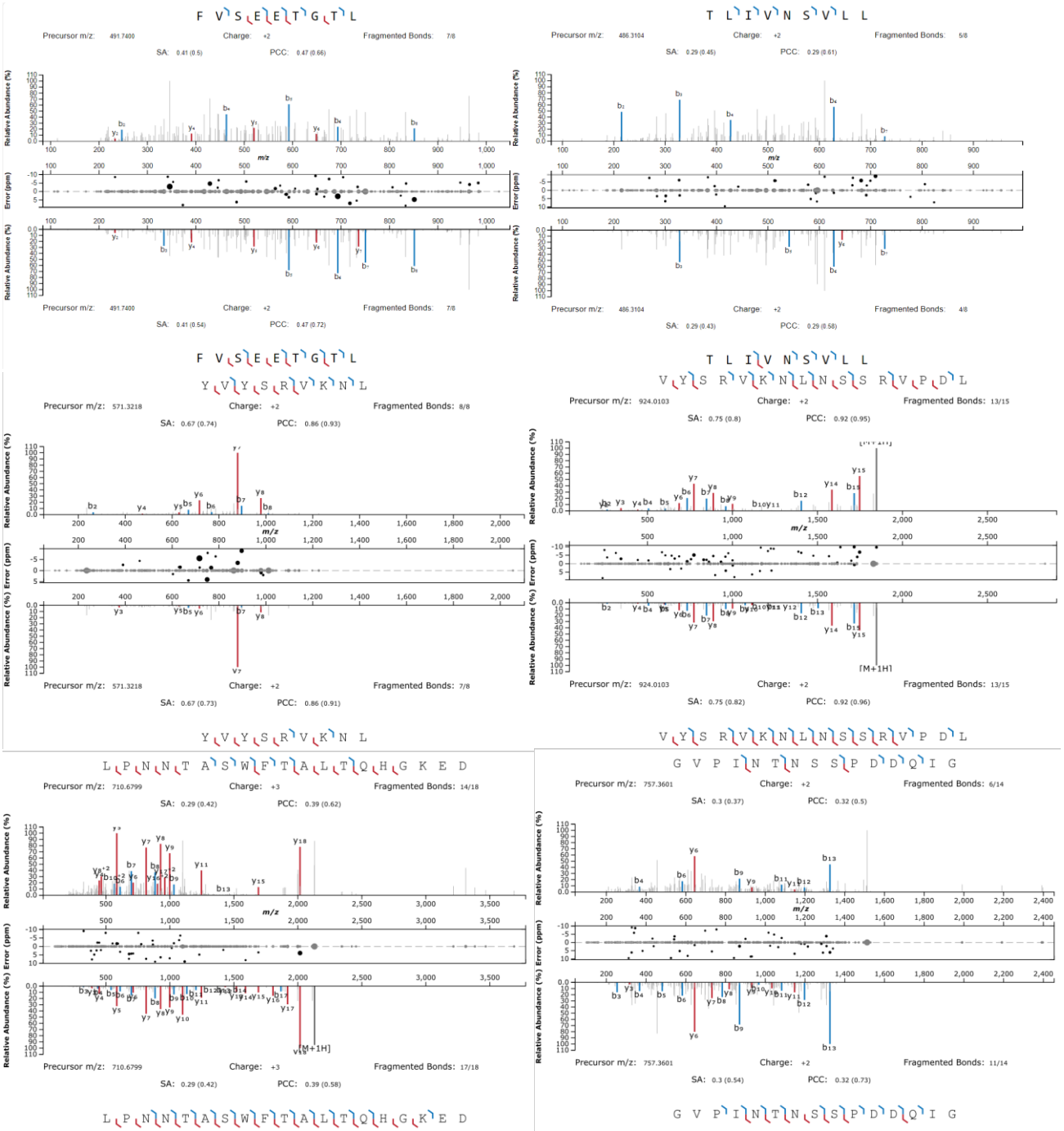

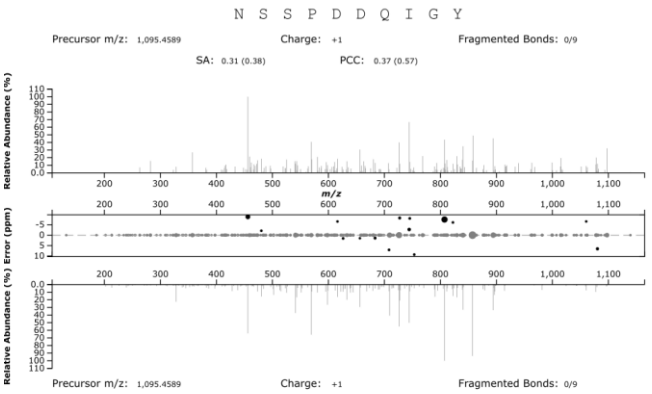
N S S P D D Q I G Y
Precursor m/z: 1,095.4589
Charge: +1
Fragmented Bonds: 0/9
SA: 0.31 (0.38)
PCC: 0.37 (0.57)
Relative Abundance (%)
m/z
Error (ppm)
Relative Abundance (%) Error (ppm)
Precursor m/z: 1,095.4589
Charge: +1
Fragmented Bonds: 0/9
SA: 0.31 (0.46)
PCC: 0.37 (0.65)

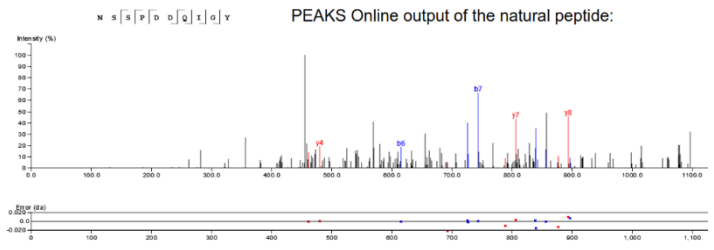
N S S P D D Q I G Y
PEAKS Online output of the natural peptide:
Intensity (%)
b7
y7
y8
y4
b6
Error (da)

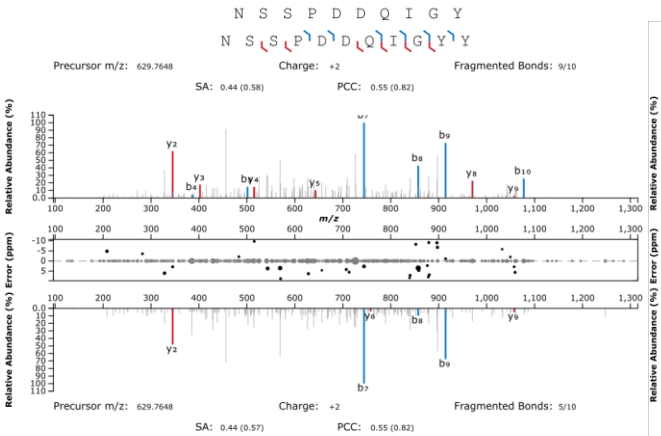
N S S P D D Q I G Y
N S S P D D Q I G Y Y
Precursor m/z: 629.7648
Charge: +2
Fragmented Bonds: 9/10
SA: 0.44 (0.58)
PCC: 0.55 (0.82)
Relative Abundance (%)
m/z
Error (ppm)
Relative Abundance (%) Error (ppm)
Precursor m/z: 629.7648
Charge: +2
Fragmented Bonds: 5/10
SA: 0.44 (0.57)
PCC: 0.55 (0.82)

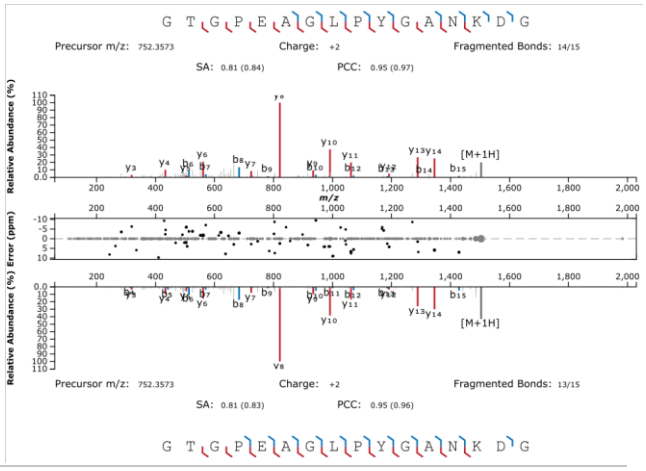
G T G P E A G L P Y G A N K D G
Precursor m/z: 752.3573
Charge: +2
Fragmented Bonds: 14/15
SA: 0.81 (0.84)
PCC: 0.95 (0.97)
[M+1H]
Relative Abundance (%)
m/z
Error (ppm)
Relative Abundance (%) Error (ppm)
Precursor m/z: 752.3573
Charge: +2
Fragmented Bonds: 13/15
SA: 0.81 (0.83)
PCC: 0.95 (0.96)

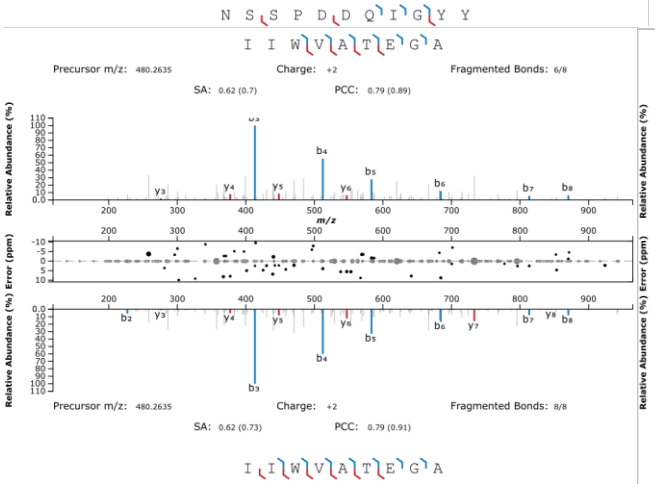
N S S P D D Q I G Y Y
I I W V A T E G A
Precursor m/z: 480.2635
Charge: +2
Fragmented Bonds: 6/8
SA: 0.62 (0.7)
PCC: 0.79 (0.89)
Relative Abundance (%)
m/z
Error (ppm)
Relative Abundance (%) Error (ppm)
Precursor m/z: 480.2635
Charge: +2
Fragmented Bonds: 8/8
SA: 0.62 (0.73)
PCC: 0.79 (0.91)

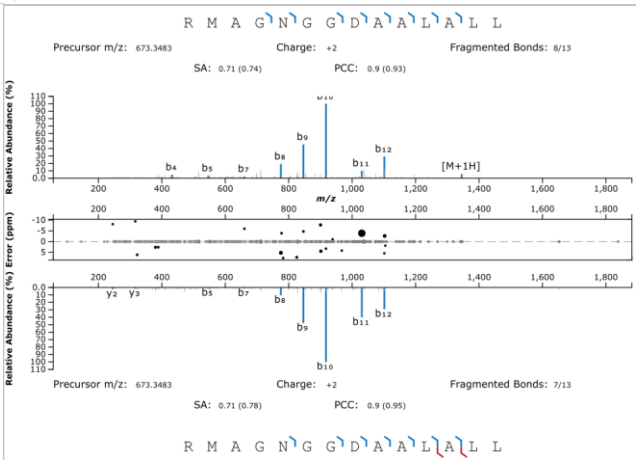
R M A G N G G D A A L A L L
Precursor m/z: 673.3483
Charge: +2
Fragmented Bonds: 8/13
SA: 0.71 (0.74)
PCC: 0.9 (0.93)
[M+1H]
Relative Abundance (%)
m/z
Error (ppm)
Relative Abundance (%) Error (ppm)
Precursor m/z: 673.3483
Charge: +2
Fragmented Bonds: 7/13
SA: 0.71 (0.78)
PCC: 0.9 (0.95)

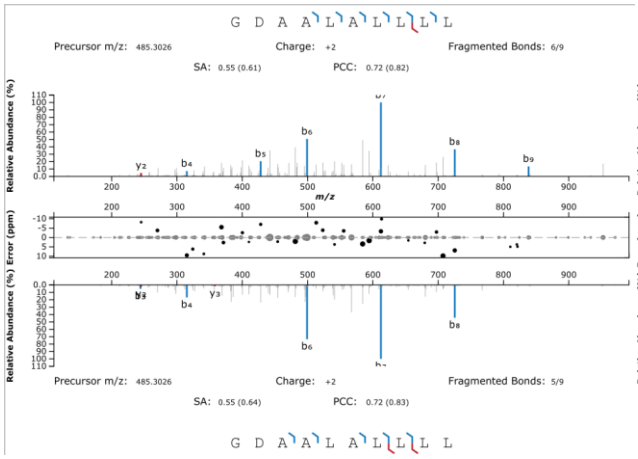
G D A A L A L L L L
Precursor m/z: 485.3026
Charge: +2
Fragmented Bonds: 6/9
SA: 0.55 (0.61)
PCC: 0.72 (0.82)
Relative Abundance (%)
m/z
Error (ppm)
Relative Abundance (%) Error (ppm)
Precursor m/z: 485.3026
Charge: +2
Fragmented Bonds: 5/9
SA: 0.55 (0.64)
PCC: 0.72 (0.83)

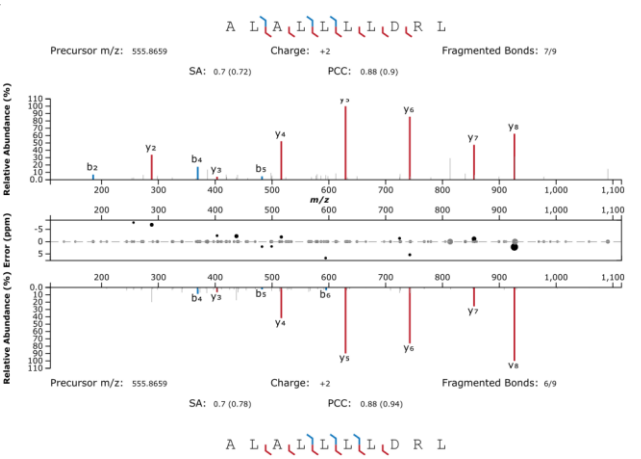
A L A L L L L D R L
Precursor m/z: 555.8659
Charge: +2
Fragmented Bonds: 7/9
SA: 0.7 (0.72)
PCC: 0.88 (0.9)
Relative Abundance (%)
m/z
Error (ppm)
Relative Abundance (%) Error (ppm)
Precursor m/z: 555.8659
Charge: +2
Fragmented Bonds: 6/9
SA: 0.7 (0.78)
PCC: 0.88 (0.94)

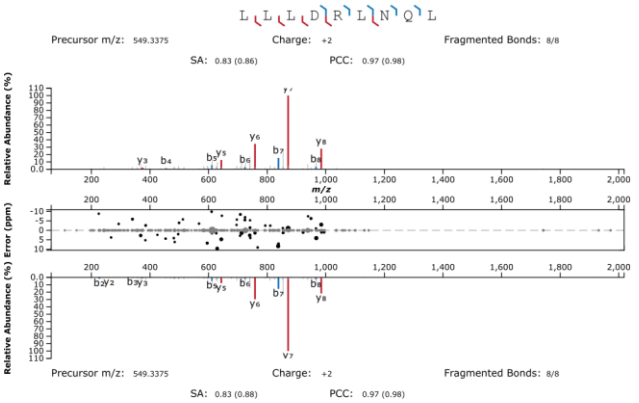

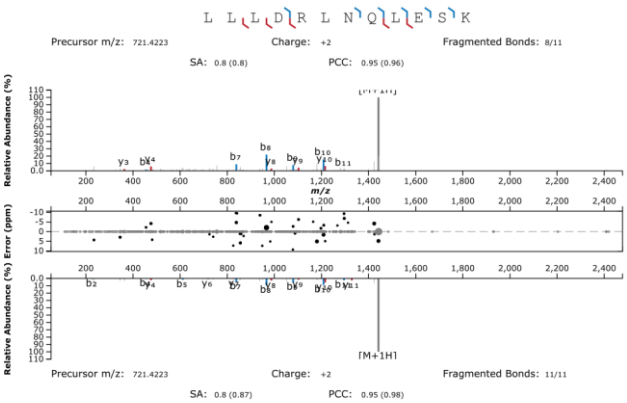

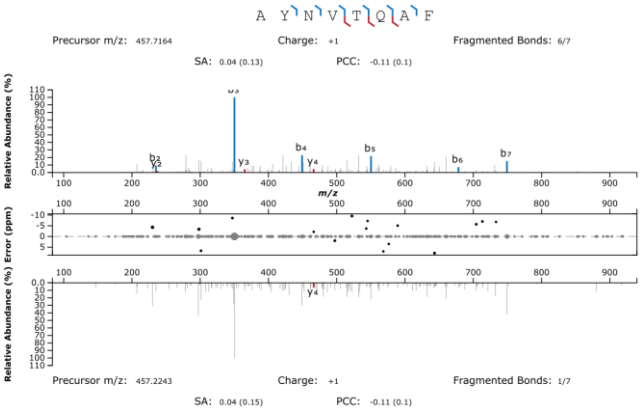

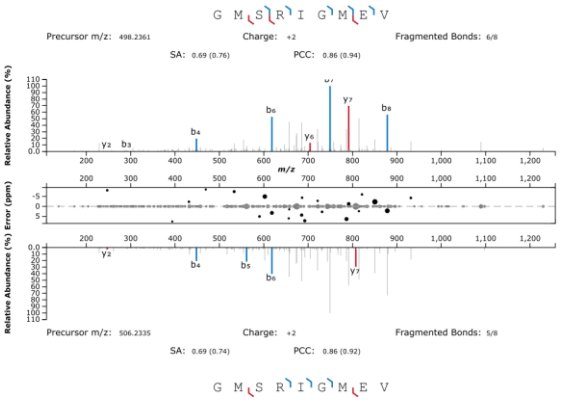

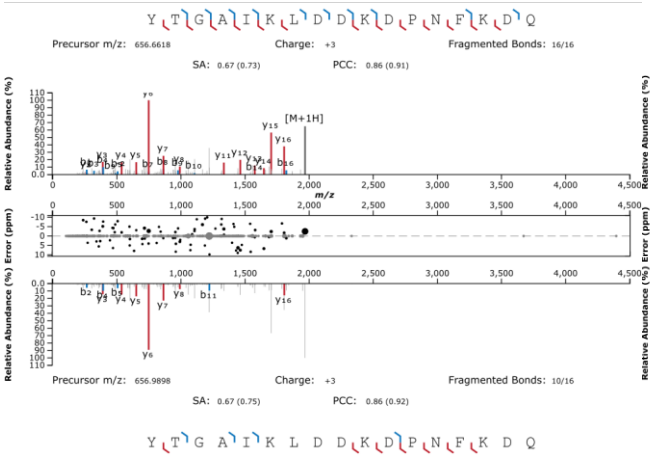

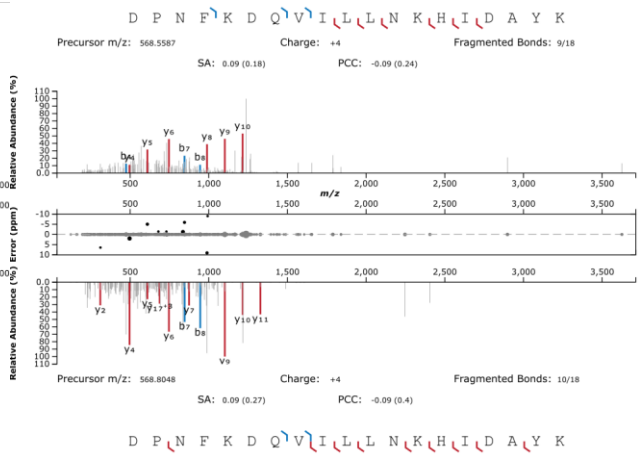

PEAKS Online output of the natural peptide:

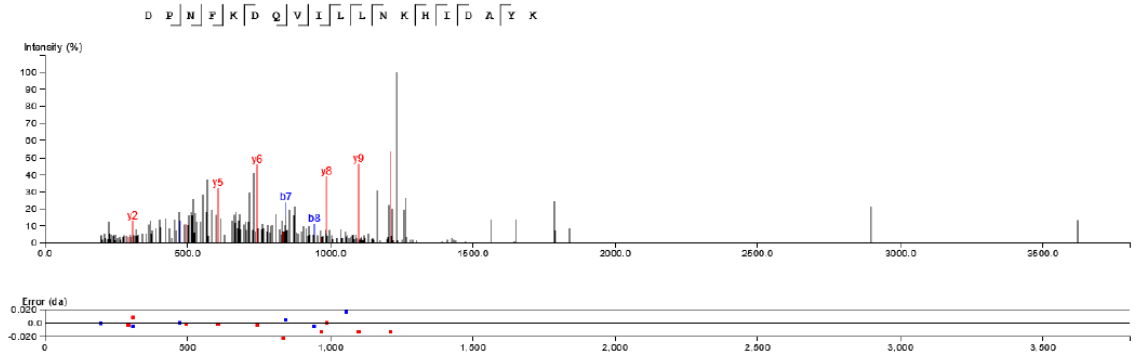

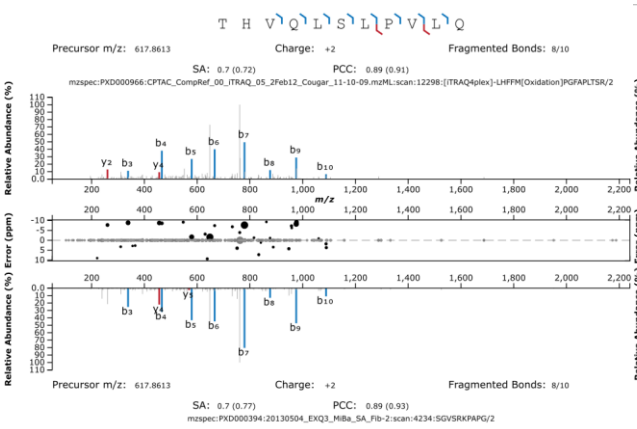

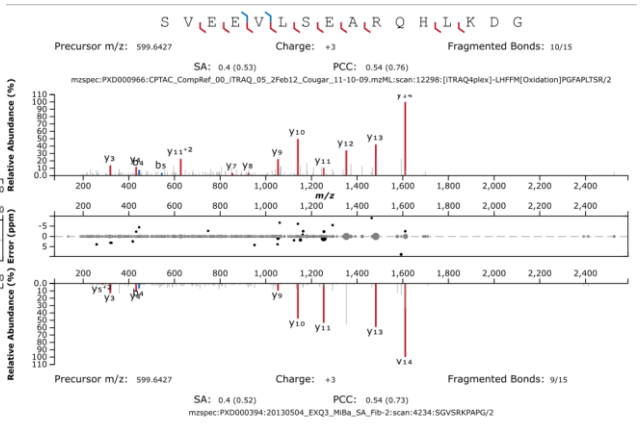

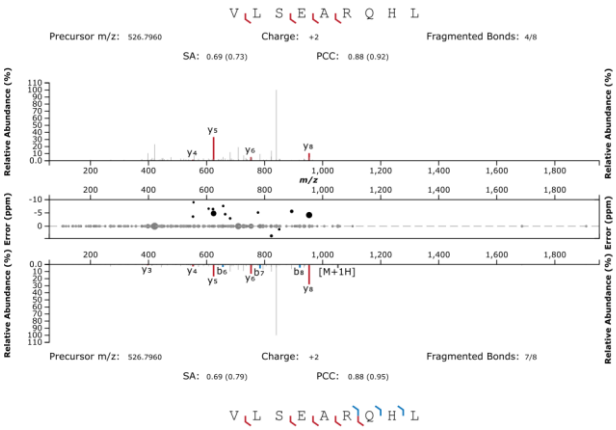

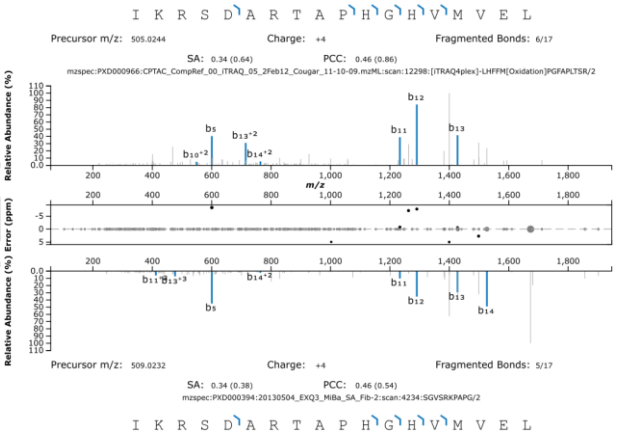

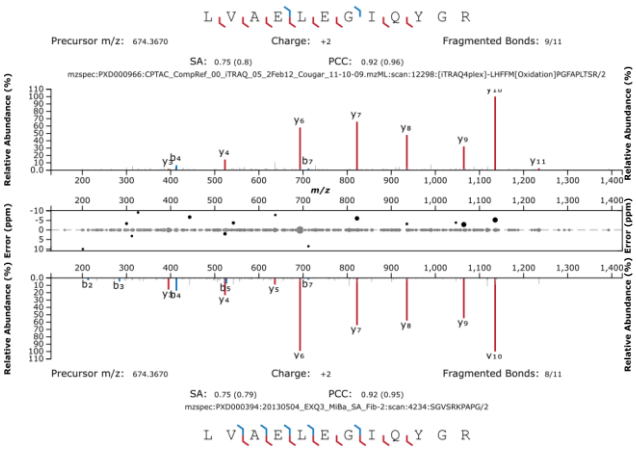

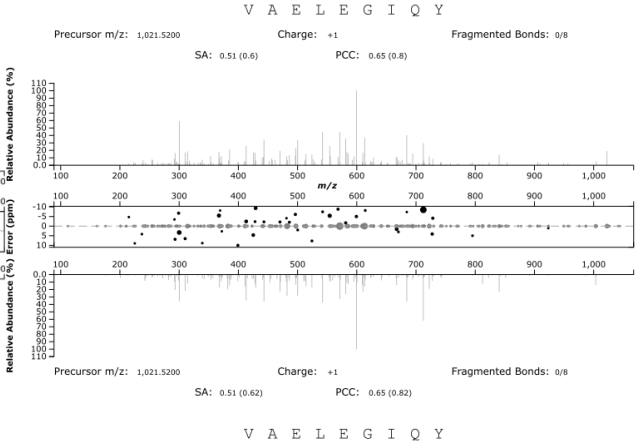

Peaks Online output of the natural peptide:

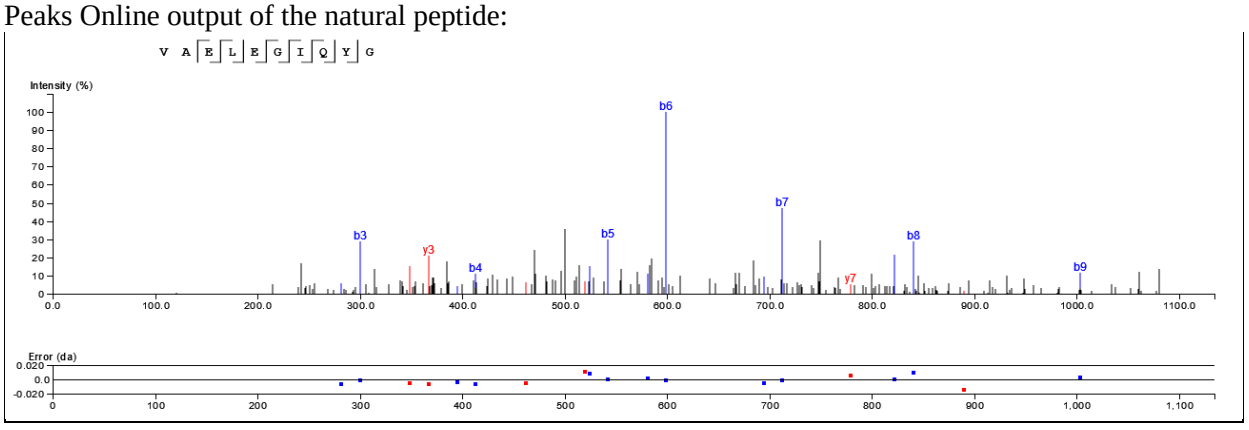

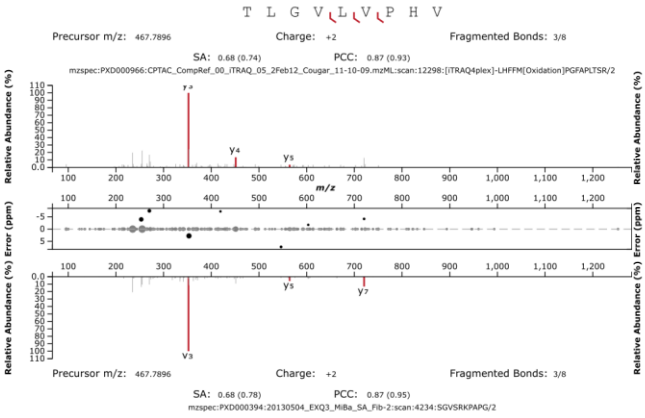

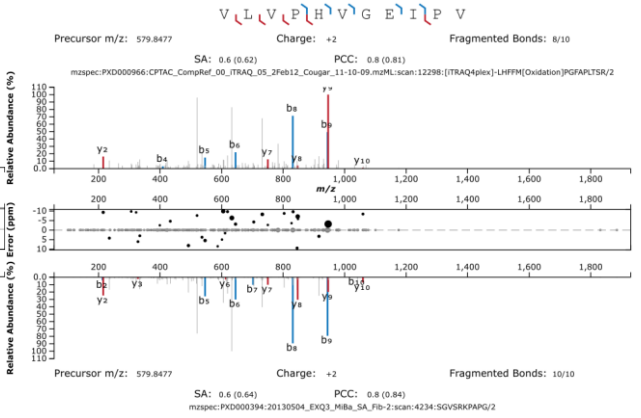

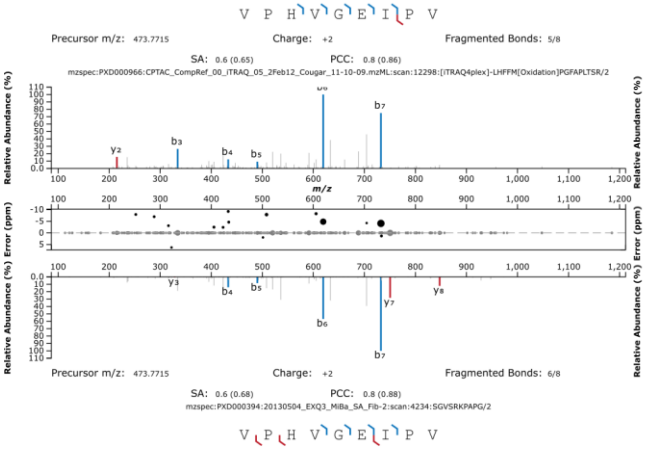

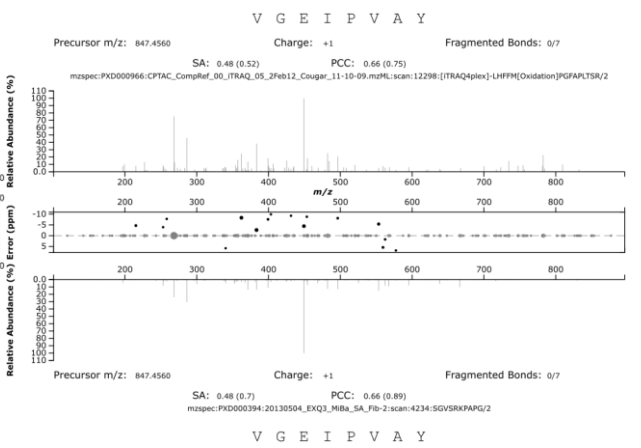

Peaks Online output of the natural peptide:

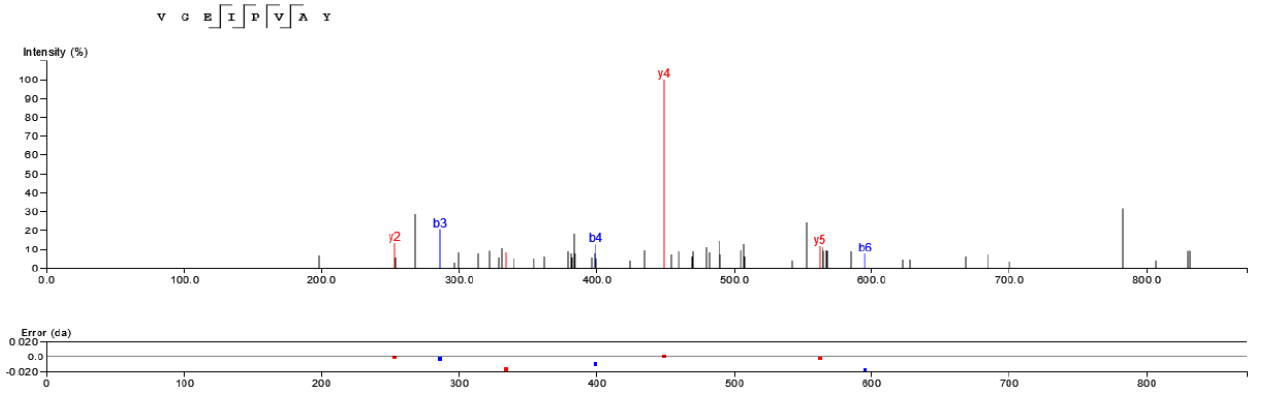

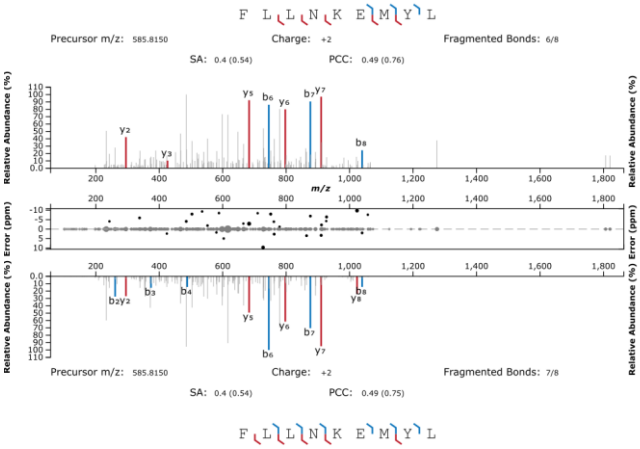

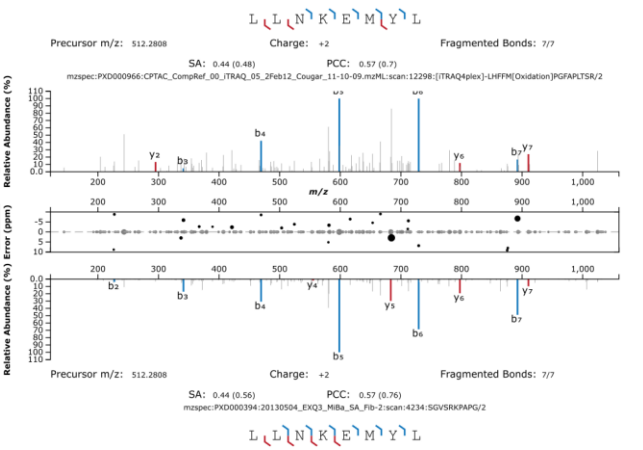

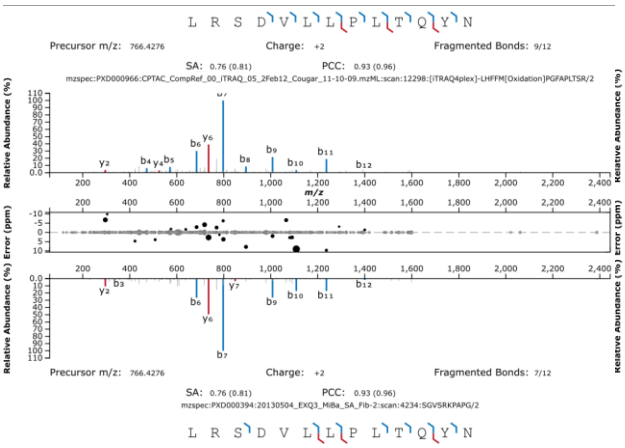

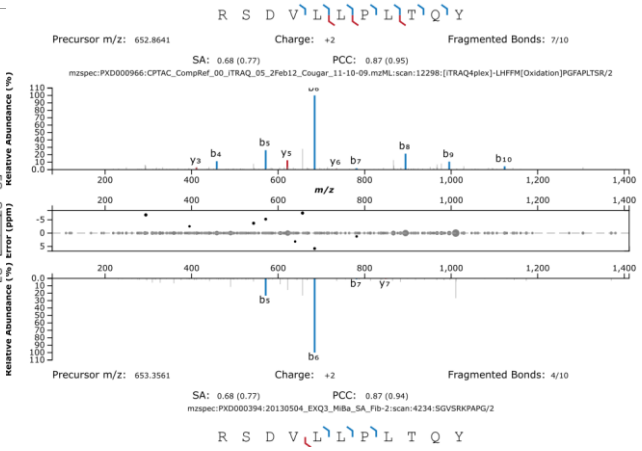

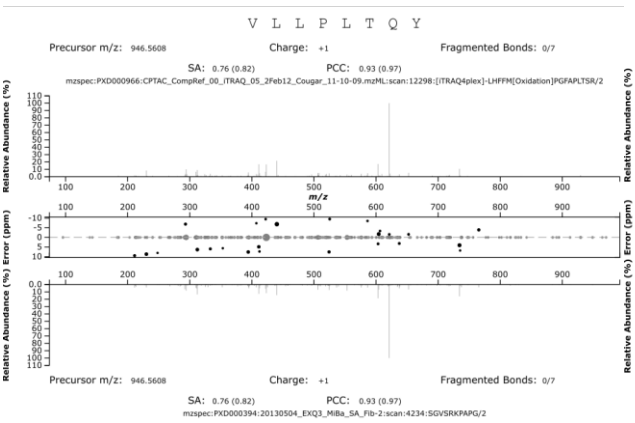

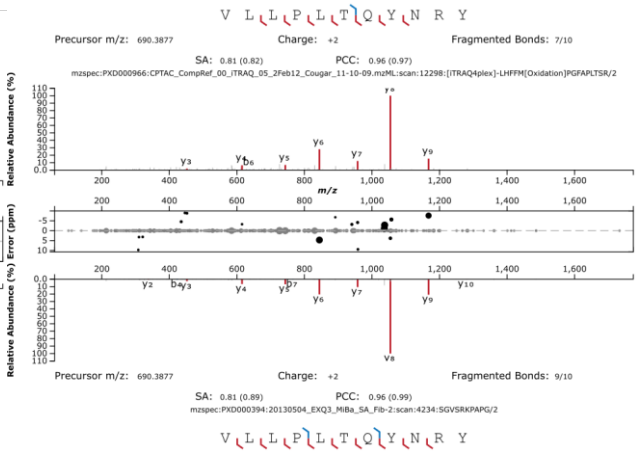

Peaks Online output of the natural peptide:

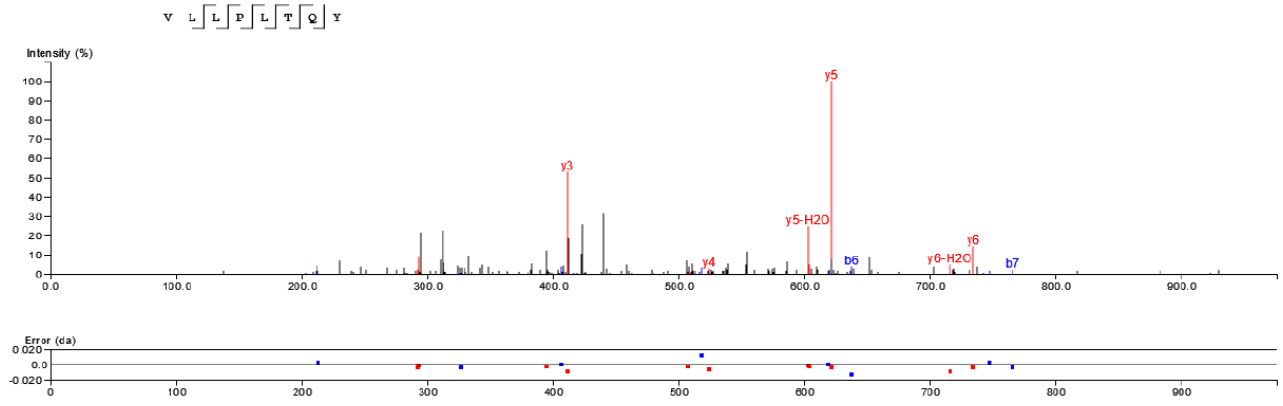

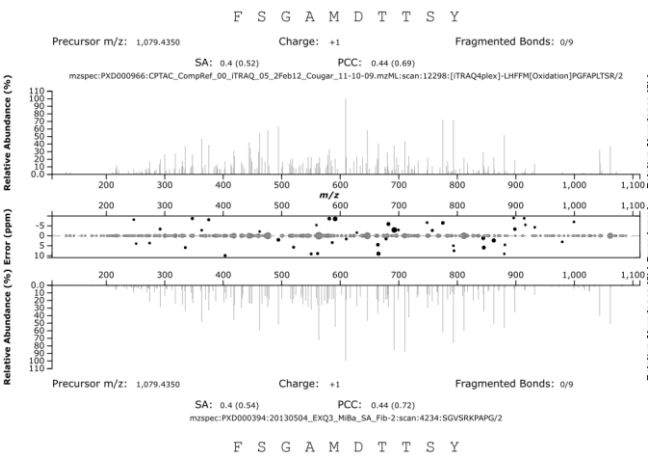

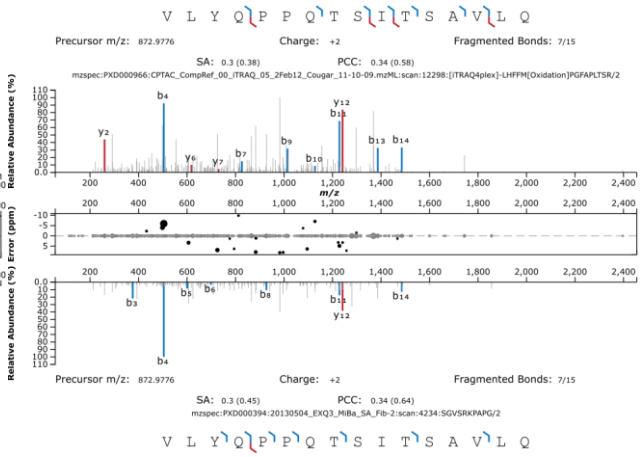

Peaks Online output of the natural peptide:

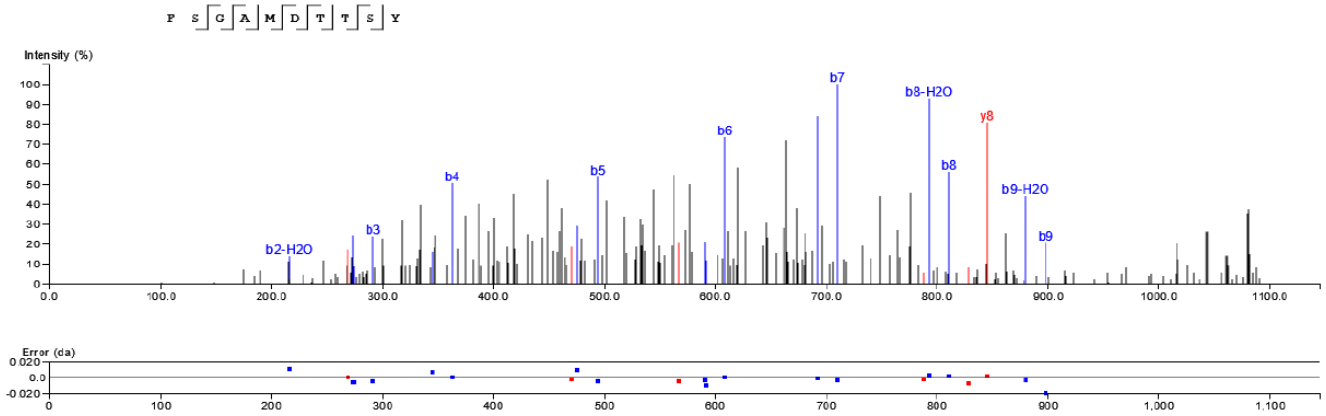

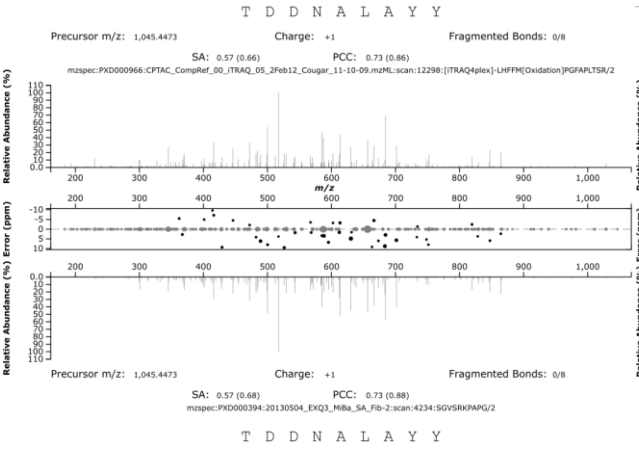

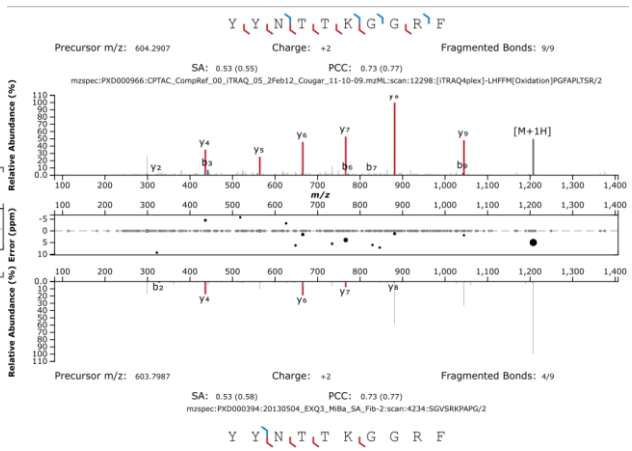

T D D N A L A Y Y

Peaks Online output of the natural peptide:

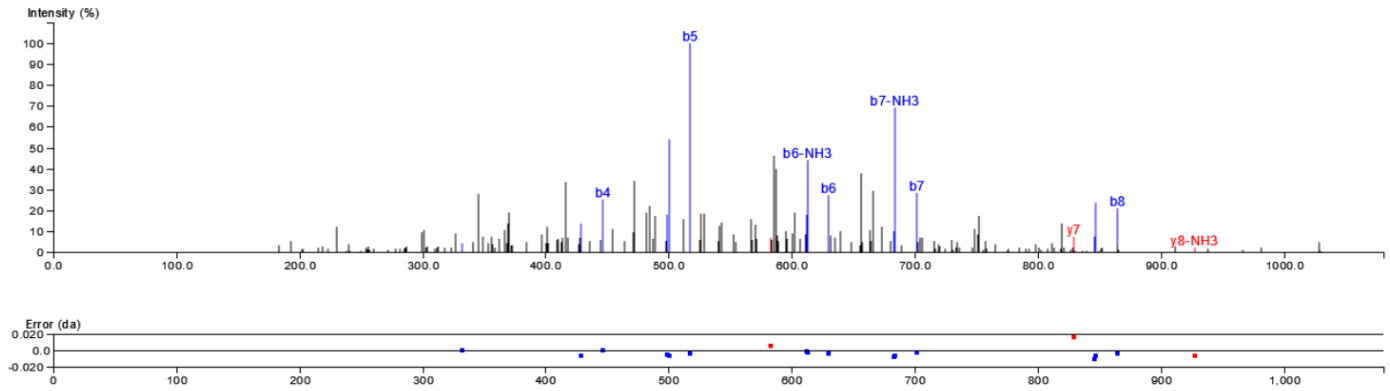

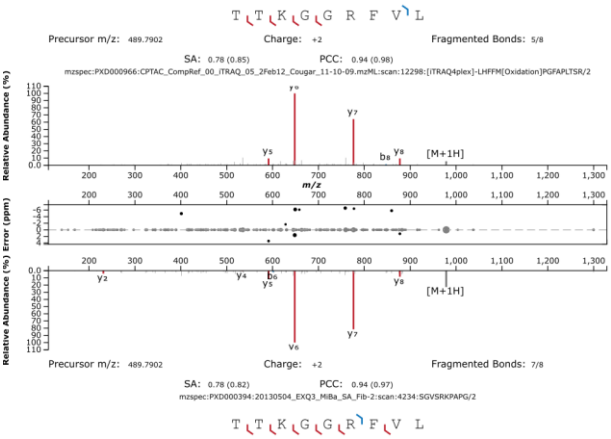

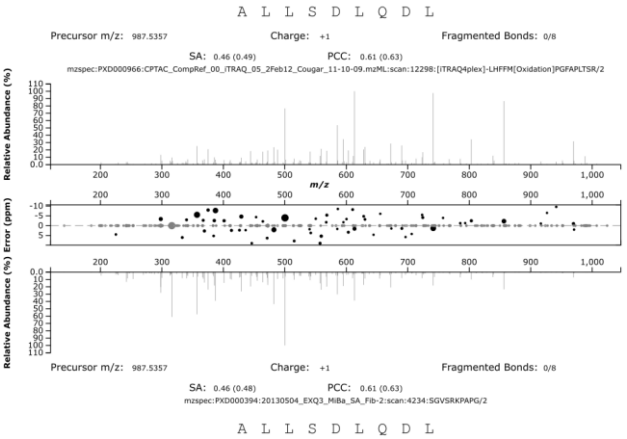

A L L S D L Q D L

Peaks Online output of the natural peptide:

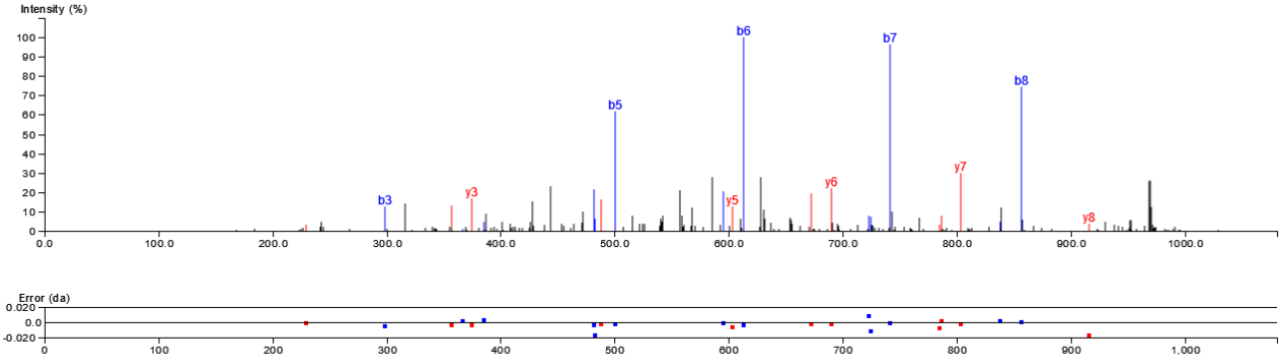

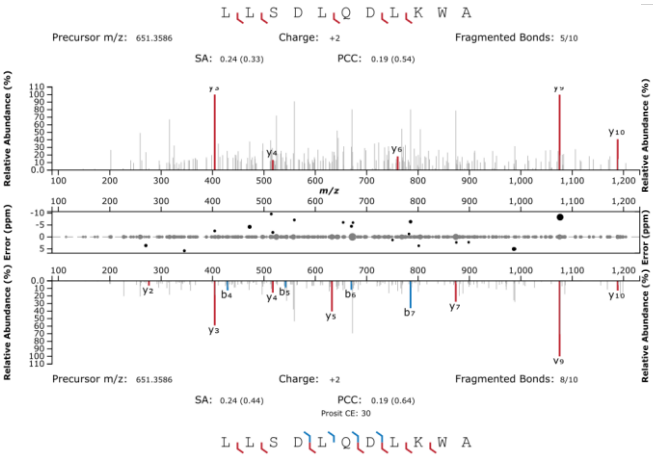

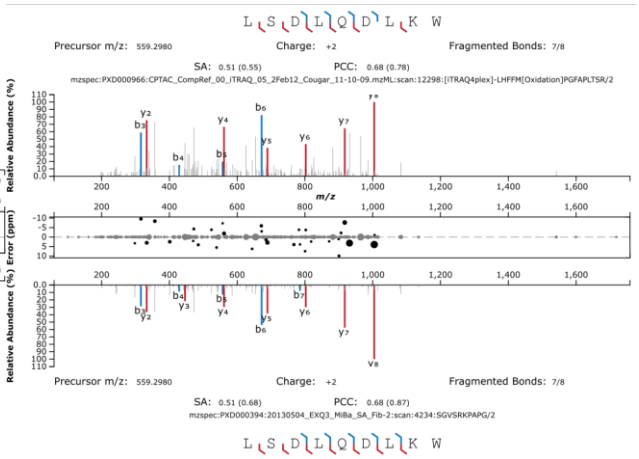

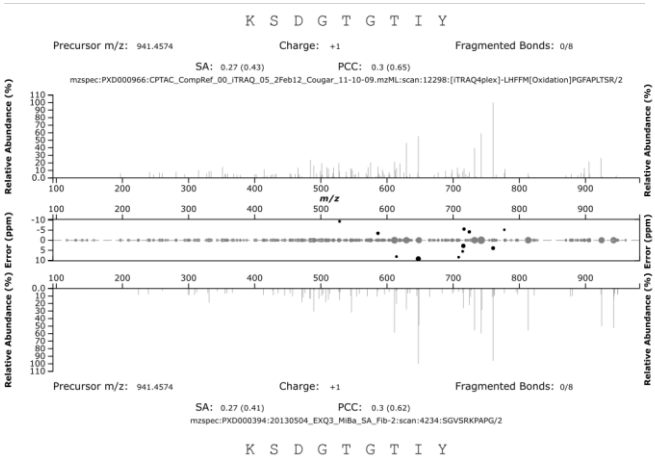

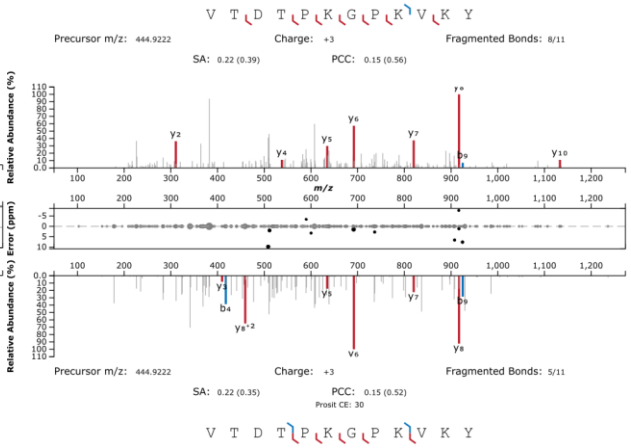

K S D G T G T I Y

Peaks Online output of the natural peptide:

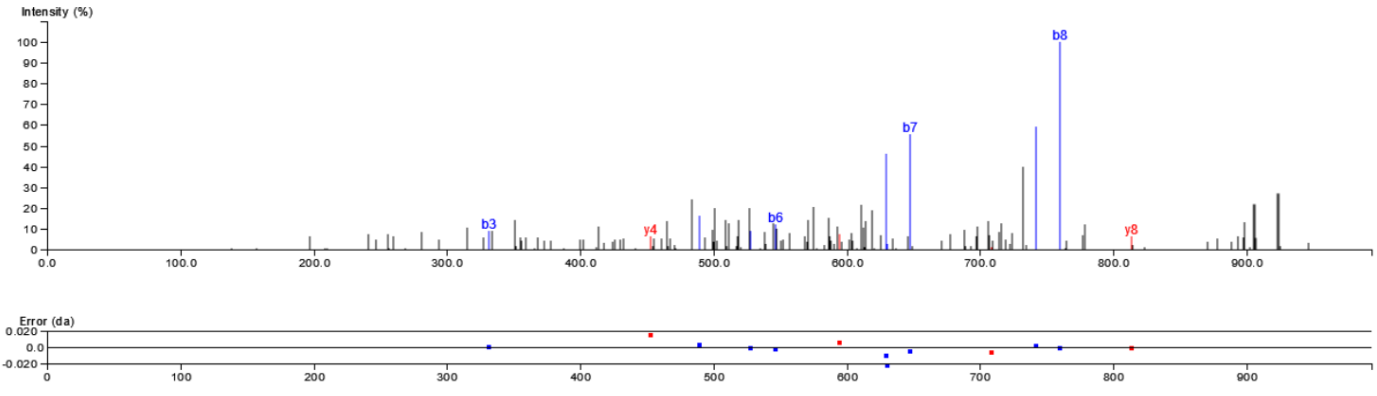

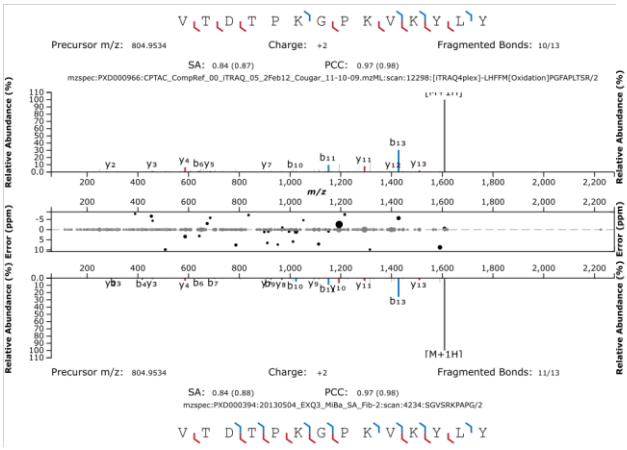

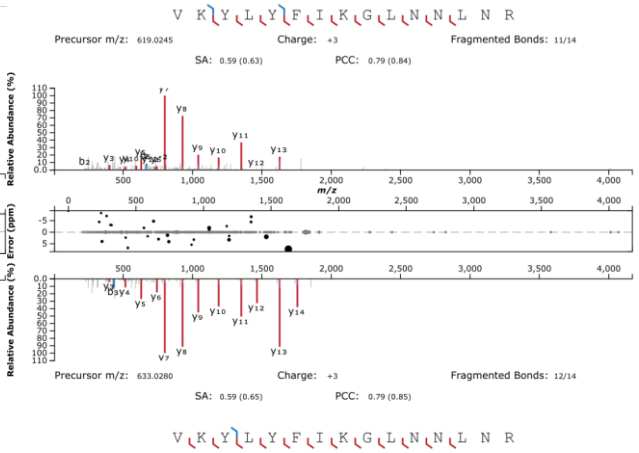

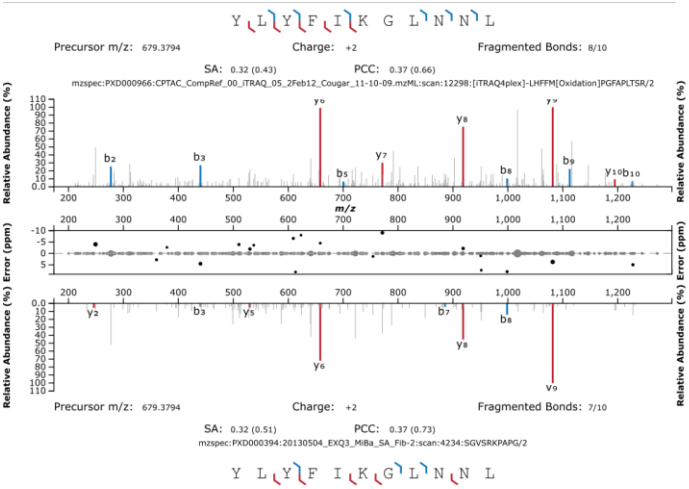

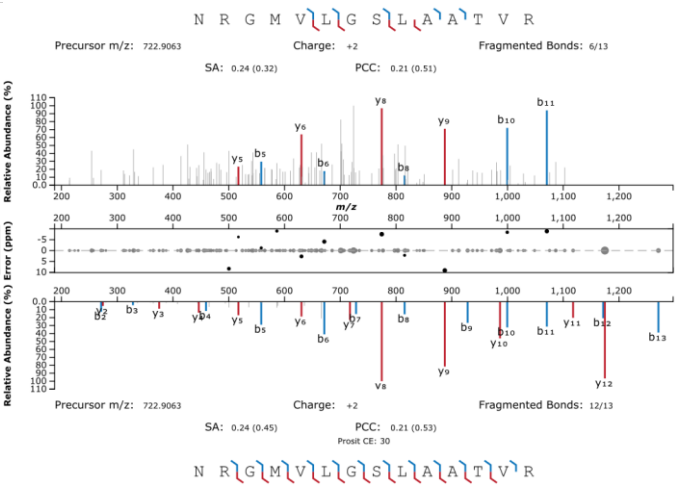

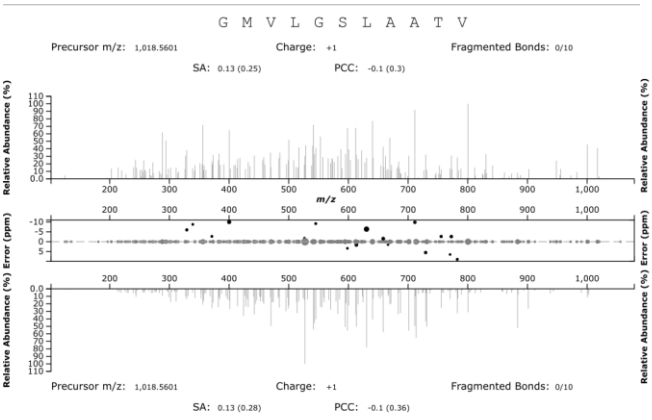

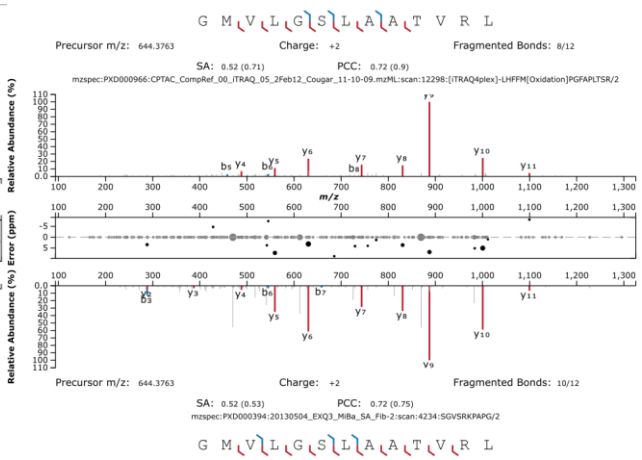

G M V L G S L A A T V

Peaks Online output of the natural peptide:

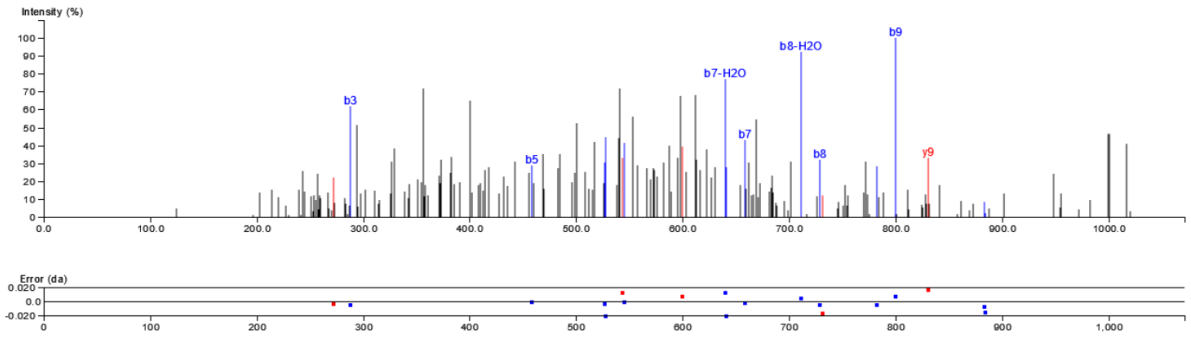

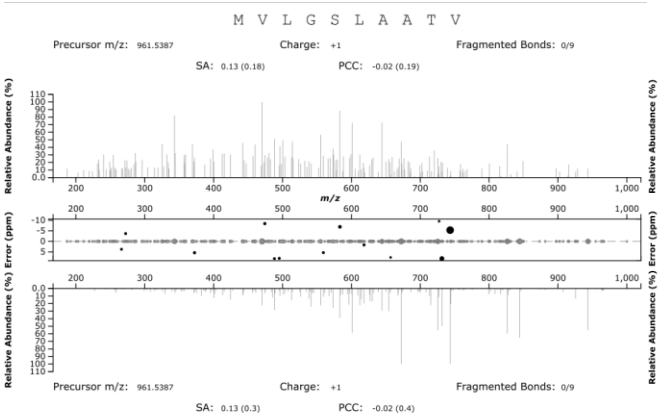

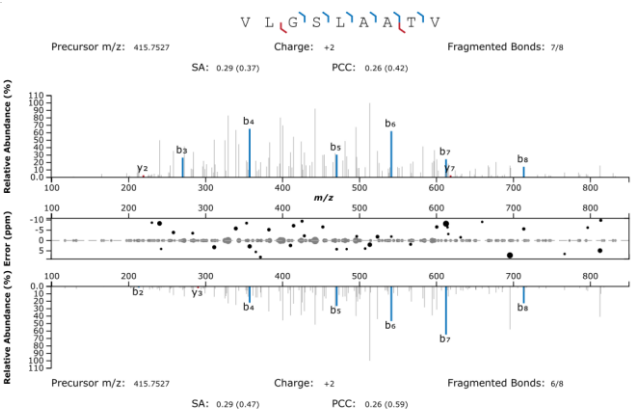

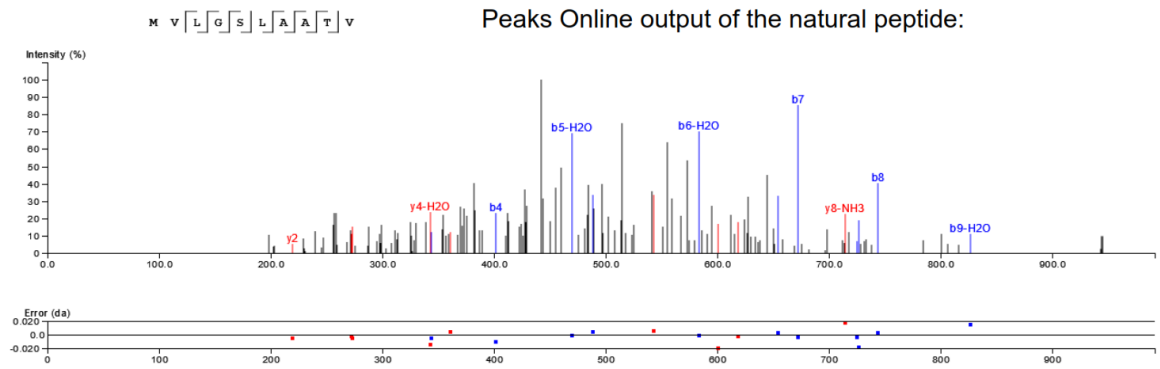

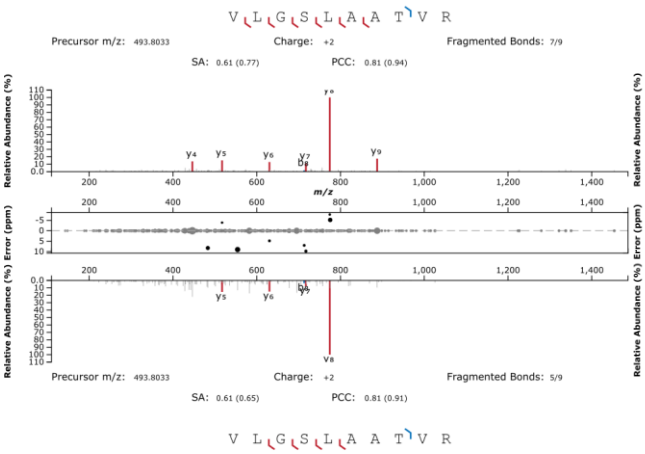

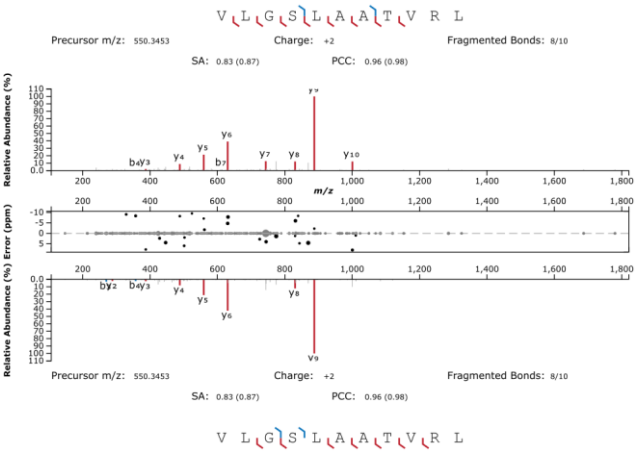

D. Mirror plots of acquired natural peptides (top) vs peptides predicted by the Prosit HLA CID model (bottom)

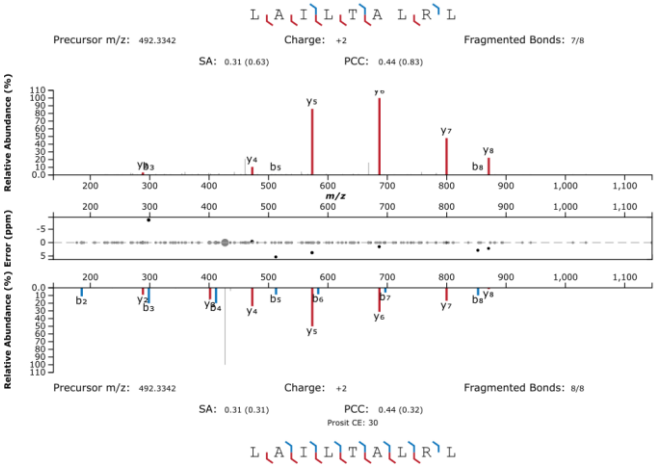

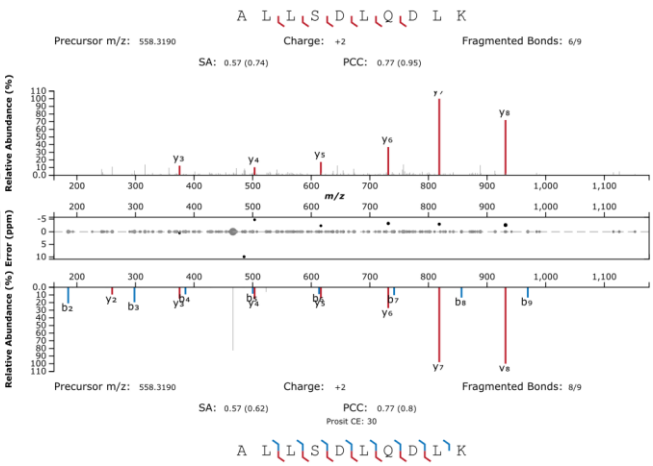

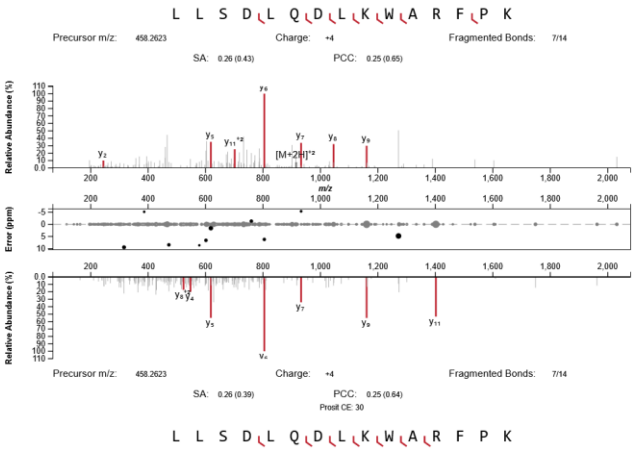

Supplemental Figure S3. Characterisation of SARS-CoV-2 peptides. (A) Detected PTM of SARS-CoV-2 derived peptides. (B) Pearson's Correlation Coefficient (PCC) of peptide spectrum matching from C-D based on best top-in-bottom or bottom-in-top value, quartiles are shown; matching of retention times including simple linear regression and error (n=59) and ion mobility including simple linear regression (n=57, 2 peptides excluded due to different charge states) of natural vs synthetic peptides. (C-D) Universal Spectrum Explorer (USE) was used to generate mirror plots comparing natural with synthetic (C) or predicted (D) peptides. For single charged peptides, where USE fails to call b- and y-ions and allocates peptides low PCC values, an additional export from the PEAKS Online search is included.

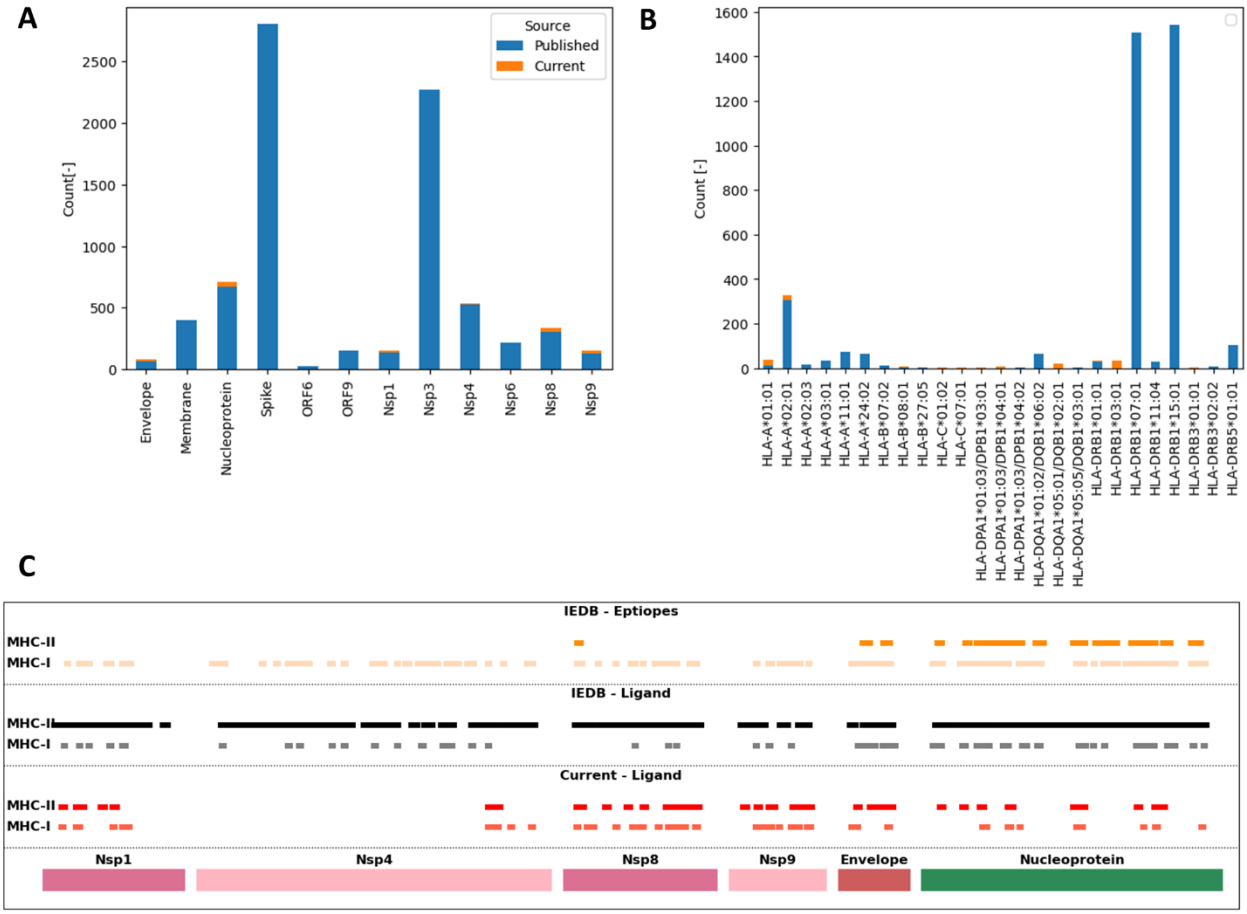

Supplemental Figure S4. Comparison of data generated in the current study and all data available in IEDB. Ligands identified by immunopeptidomics in the current study were compared to fluorescence binding assays (n=6211), high-throughput multiplex assays (n=5703) and MS based ligandomics (n=378) deposited in the Immune Epitope Database (IEDB) for SARS-CoV-2 reading frames (A) and HLA restriction (B). The same data represented as an alignment to source proteins shows the ligand coverage of proteins analysed in the current study and the coverage from the data annotated in IEDB, divided by MHC Class I or II restriction (C). Nsp: non-structural protein, HLA: human leukocyte antigen, MHC: Major histocompatibility complex.

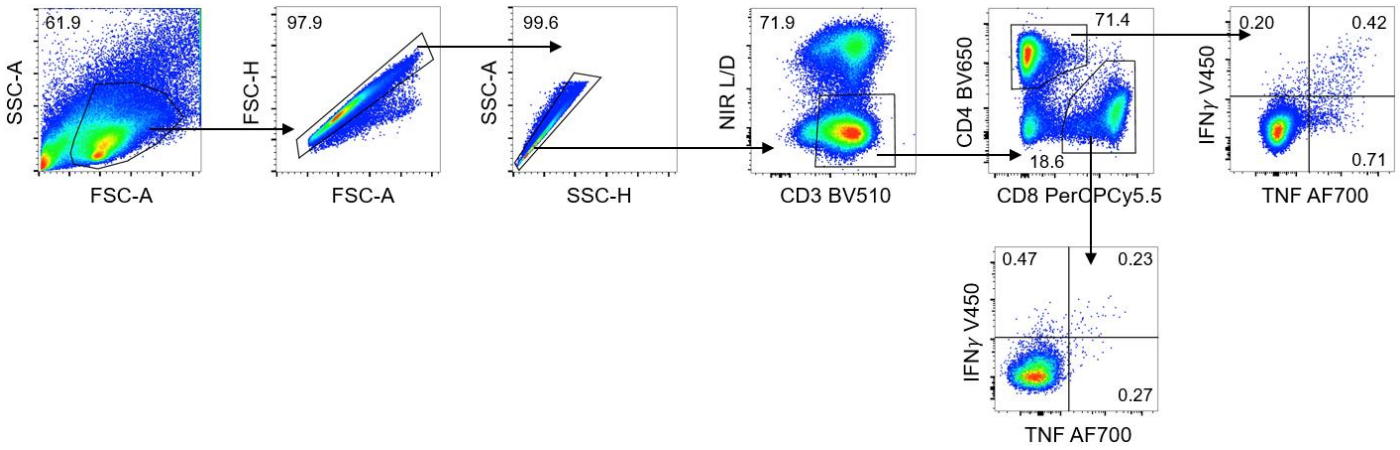

Supplemental Figure S5. Flow cytometry gating. Gating strategy for the intracellular staining assay to measure peptide responses.

References

1. Solberg, O.D., et al., *Balancing selection and heterogeneity across the classical human leukocyte antigen loci: a meta-analytic review of 497 population studies.* Hum Immunol, 2008. **69**(7): p. 443-64.